

PMRNet: Physics-informed Multi-scale Refinement Network for Medical Image Segmentation

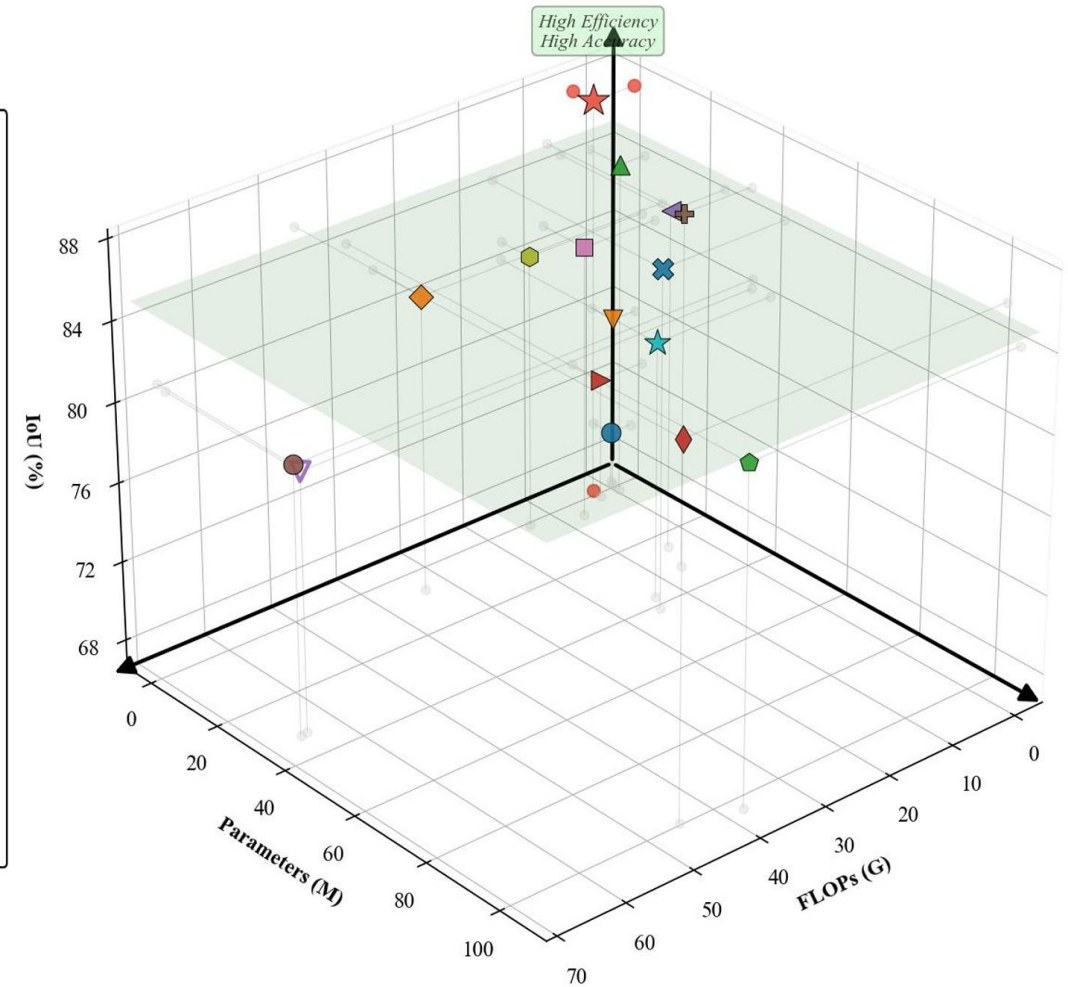
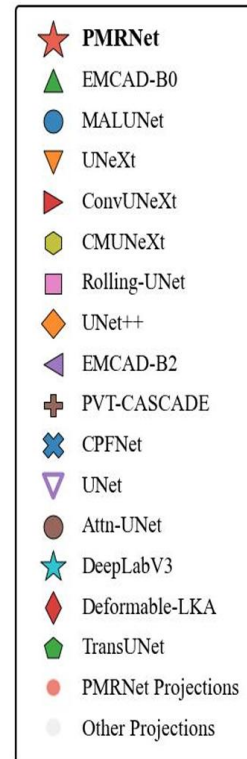
Boce Kang

Northwestern Polytechnical University

CVPR 2026

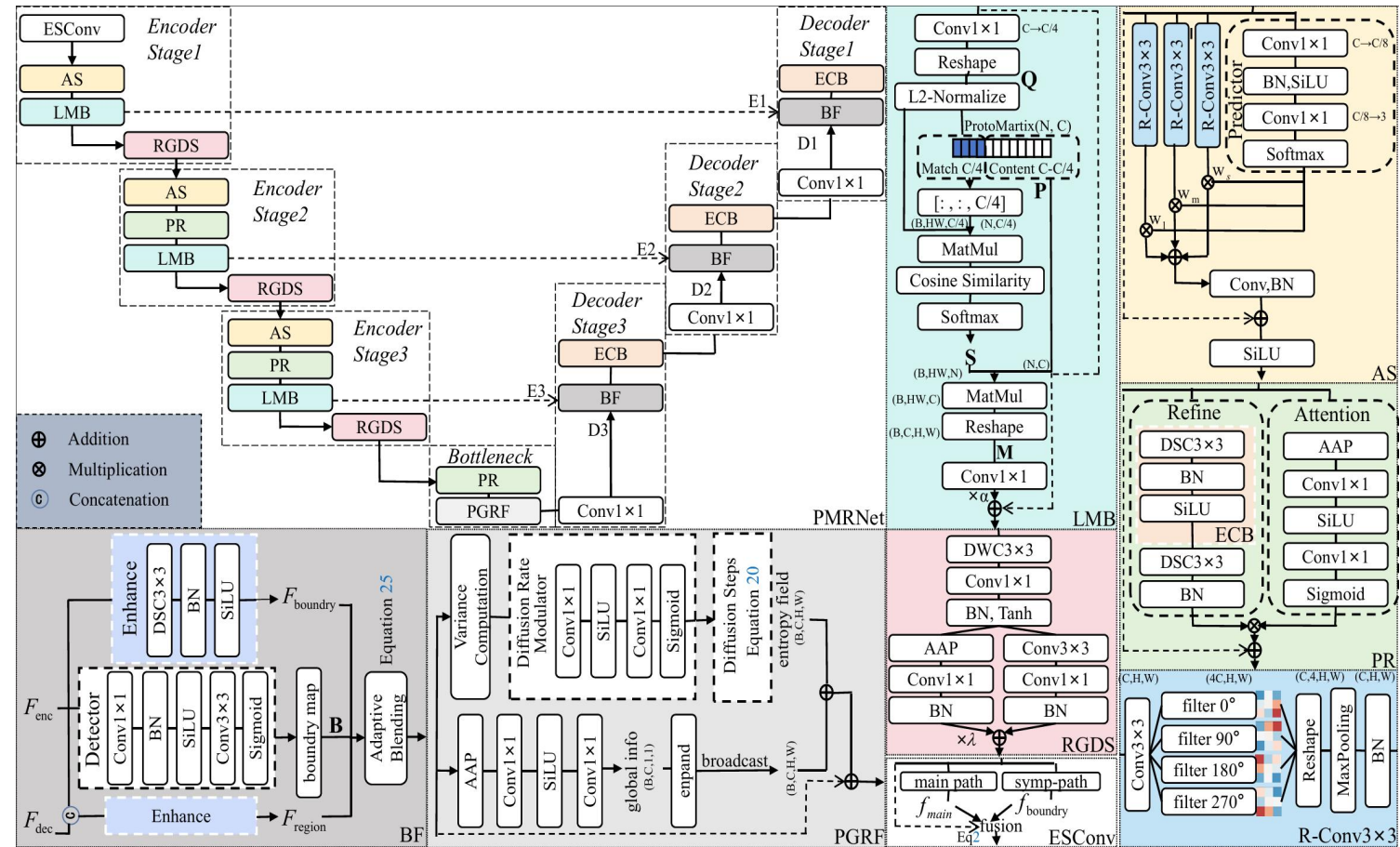
Background & Motivation

- Clinical Need: Point-of-care medical image segmentation requires both high accuracy and computational efficiency.
- The Dilemma:
- CNNs lack global context.
- Transformers are too computationally expensive.
- Existing lightweight models sacrifice accuracy on complex structures.
- Our Goal: Achieve SOTA accuracy with <1M parameters.



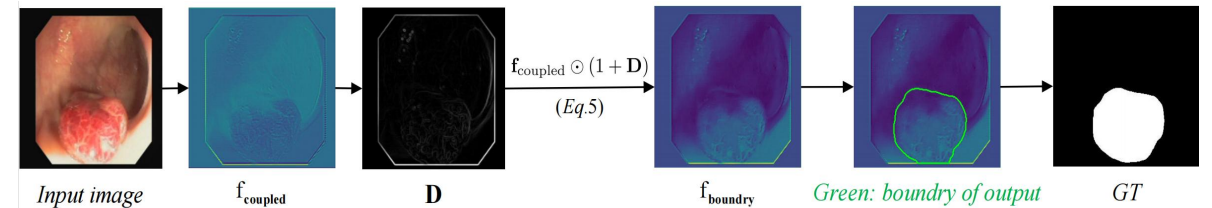
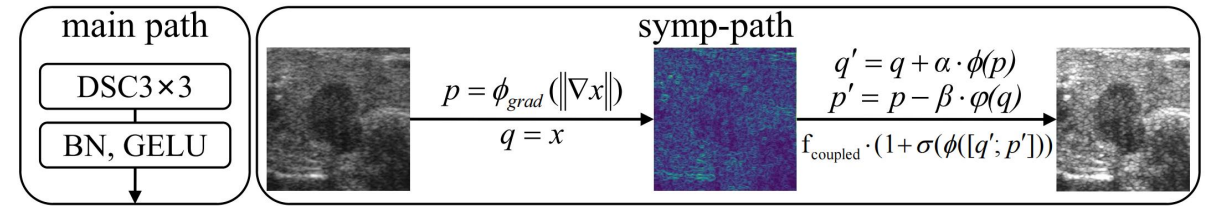
Proposed Solution: PMRNet Overview

- Instead of scaling up parameters, we scale up inductive bias using physics principles.
- Three Key Innovations:
 1. Physics-informed Encoder
 2. Efficient Global Context (Entropy-driven Diffusion)
 3. Boundary-aware Decoder



Innovation: Enhanced Symplectic Convolution

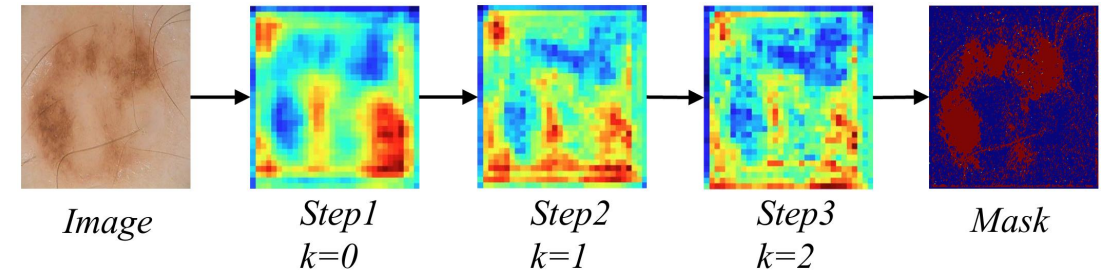
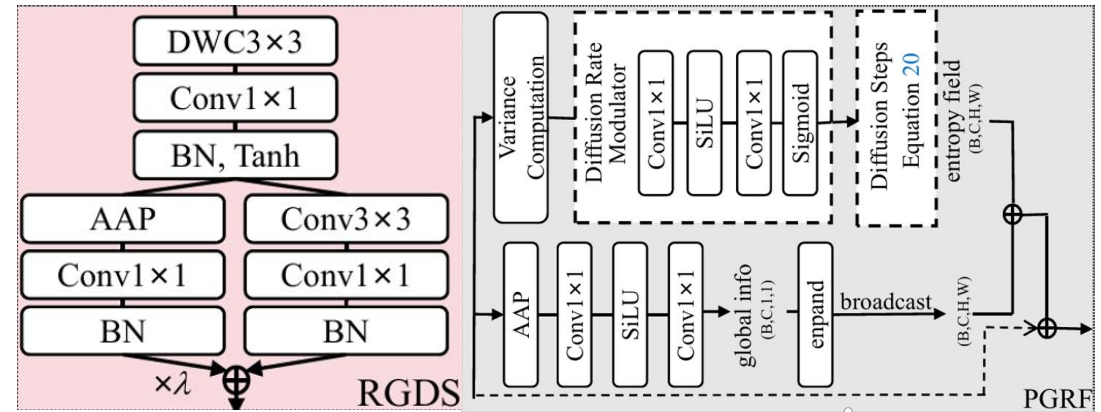
- Problem: Standard convolutions treat boundaries and interiors identically.
- Solution: Inspired by Hamiltonian mechanics.
- Feature maps = Position (q)
- Spatial gradients = Momentum (p)
- Mechanism: Couples spatial features with derivatives in a joint update step.
- Result: Preserves boundary signals without heavy attention mechanisms.



$$\begin{bmatrix} \mathbf{q}' \\ \mathbf{p}' \end{bmatrix} = \begin{bmatrix} \mathbf{q} \\ \mathbf{p} \end{bmatrix} + \epsilon \cdot \tanh(\text{BN}(\text{Conv}_{1 \times 1}([\mathbf{p}; -\mathbf{q}])))$$

Innovation: PGRF & RGDS

- Pseudo-Global Receptive Field (PGRF):
- Replaces $O(N^2)$ self-attention with $O(N)$ heat equation diffusion.
- Information flows adaptively from high-certainty to uncertain areas.
- Renormalization Group Downsampling (RGDS):
- Folds fine-scale structures into channels before halving resolution.
- Prevents loss of small object information.

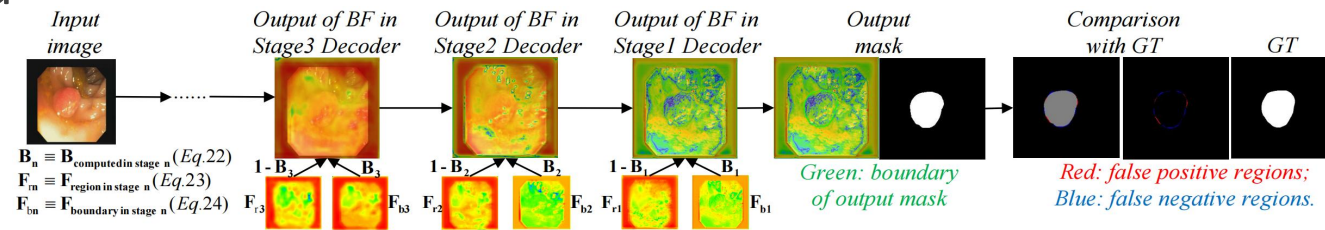
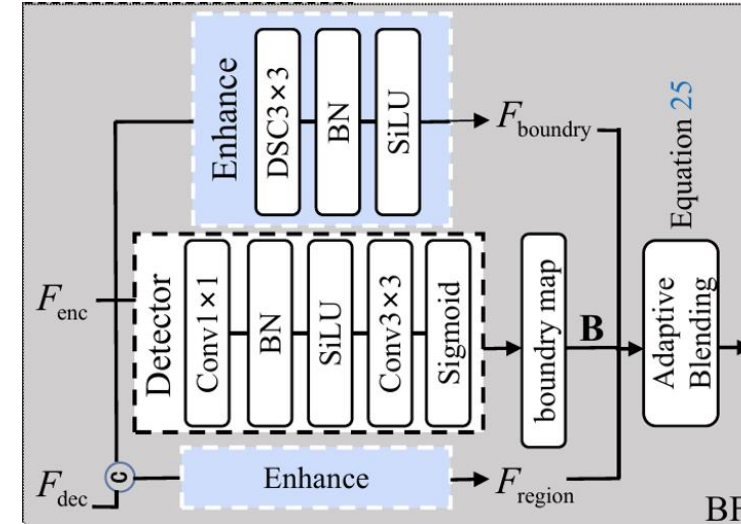


$$\mathbf{x}_{\text{enhanced}} = \mathbf{x} + \alpha \cdot (\beta(\mathbf{x}) + \gamma(\mathbf{x}) \odot \mathbf{x})$$

$$\mathbf{u}^{(k+1)} = \mathbf{u}^{(k)} + D(\mathbf{x}) \odot \mathcal{L}(\mathbf{u}^{(k)}) \cdot (0.5)^k + 0.1 \cdot \mathbf{g}$$

Innovation: Boundary-aware Decoder

- Concept: Not all skip connections are equally useful.
- Boundary-aware Fusion (BF) Module:
- Gates skip connections based on learned local boundary strength.
- Region path & Boundary path processed separately.
- Result: Keeps the decoder spatially precise with minimal parameters.



Results: Computational Efficiency

- Ultra-lightweight footprint:
- Parameters: 0.87M (100x smaller than TransUNet)
- Computations: 3.43 GFLOPs
- Real-time Inference:
- Achieves 152.03 FPS on a single RTX 4090.
- Outperforms heavier models while maintaining strict computational budgets.

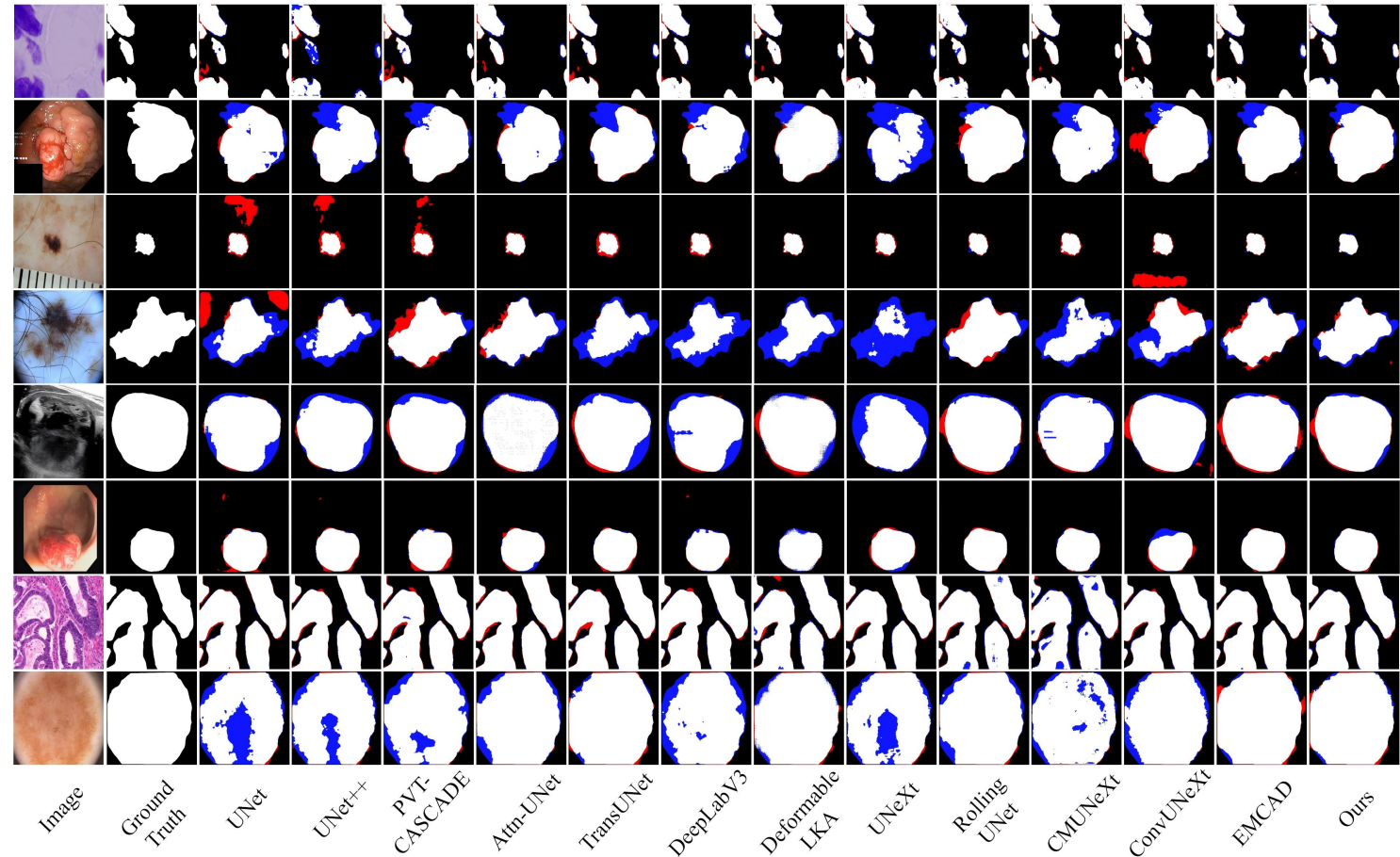
Method	Params(M)	FLOPs(G)	TG3K							Clinic								
			IoU↑	Dice↑	HD95↓	ASD↓	SE↑	PC↑	SP↑	ACC↑	IoU↑	Dice↑	HD95↓	ASD↓	SE↑	PC↑	SP↑	ACC↑
UNet [51]	34.53	65.53	71.20	80.90	23.19	7.81	83.81	83.63	98.83	97.43	80.00	87.26	21.61	6.63	87.33	91.16	99.11	98.21
UNet++ [74]	9.16	34.65	72.47	81.55	20.14	7.58	83.94	85.07	98.94	97.57	82.05	88.84	23.85	5.86	90.74	89.41	99.01	98.33
TransUNet [9]	105.32	38.52	73.22	82.24	20.97	7.07	84.69	84.94	98.72	97.46	83.87	90.35	16.72	4.27	91.14	91.48	99.25	98.50
UNeXt [61]	1.47	0.57	70.64	80.06	19.19	7.19	84.44	82.16	98.56	97.45	75.75	84.40	29.48	6.84	85.99	87.09	98.94	97.92
Rolling-UNet [40]	7.10	8.28	72.09	81.20	18.10	6.71	83.84	83.69	98.81	97.49	80.98	87.82	19.55	5.63	88.75	89.63	99.15	98.43
PVT-CASCADE [49]	34.12	7.62	73.77	82.75	17.34	5.93	86.32	83.97	98.67	97.44	85.09	91.07	14.94	4.38	91.10	92.03	99.34	98.77
Attn-UNet [45]	34.88	66.64	73.29	82.11	19.01	7.40	83.66	86.20	99.01	97.56	80.52	87.46	23.03	7.17	88.43	90.21	99.06	98.18
Deformable-LKA [3]	101.64	46.12	73.04	82.25	17.94	5.99	85.30	83.30	98.64	97.60	85.65	91.60	13.90	3.57	92.19	92.15	99.18	98.70
DeepLabV3 [10]	39.76	14.92	66.21	76.92	19.93	7.76	79.09	81.30	98.74	97.12	80.09	87.50	19.48	6.47	89.17	87.63	99.00	98.30
CPFNet [19]	43.27	16.15	73.89	83.02	16.10	5.67	85.43	84.90	98.76	97.60	84.26	90.70	16.24	4.02	91.72	91.26	99.16	98.58
EMCAD-B2 [50]	26.76	5.60	74.88	83.56	15.49	5.75	86.35	84.59	98.75	97.83	84.30	90.47	14.47	4.31	90.61	92.35	99.35	98.71
CMUNeXt [60]	3.15	14.84	69.48	79.13	19.91	8.05	82.28	83.20	98.61	97.17	80.97	87.92	21.16	6.72	89.07	89.95	98.90	98.19
EMCAD-B0 [50]	3.92	0.84	70.83	80.43	20.01	7.08	82.87	84.34	98.75	97.18	83.98	90.52	16.35	4.45	90.39	91.80	99.36	98.68
MALUNet [52]	0.18	0.17	66.67	77.00	20.63	7.66	81.18	79.11	98.24	96.78	69.59	79.69	29.20	8.94	82.52	81.18	98.52	97.18
ConvUNeXt [23]	3.54	3.69	64.76	74.93	22.72	8.76	78.15	79.62	98.58	96.82	73.20	81.50	26.12	9.10	82.14	85.07	98.82	97.78
PMRNet (Ours)	0.87	3.43	76.19	84.73	14.96	5.51	86.03	87.61	98.97	97.85	87.25	92.56	13.13	3.54	93.40	92.50	99.38	98.98

Method	Breast			BUSI			DDTI			DSB18			GlaS		
	IoU↑	Dice↑	HD95↓	IoU↑	Dice↑	HD95↓	IoU↑	Dice↑	HD95↓	IoU↑	Dice↑	HD95↓	IoU↑	Dice↑	HD95↓
UNet	60.53	71.55	40.35	64.74	74.24	36.76	80.18	88.64	20.48	85.83	92.07	3.68	82.73	90.13	25.91
UNet++	61.70	72.48	38.11	67.89	76.91	35.52	80.30	88.75	19.21	85.15	91.59	3.98	84.79	91.46	21.18
TransUNet	62.64	72.67	29.52	69.06	78.22	28.67	80.80	89.11	19.63	86.25	92.26	3.40	83.98	90.83	24.37
Rolling-UNet	63.64	73.65	31.82	71.55	80.78	26.64	79.06	87.94	20.34	84.84	91.42	4.04	84.59	91.29	23.25
EMCAD-B2	64.72	74.82	30.38	72.03	80.61	22.69	82.27	90.02	16.98	85.33	91.71	3.83	85.39	91.79	21.44
Deformable-LKA	38.27	51.09	67.32	71.83	80.63	23.33	82.81	90.30	16.07	85.86	92.00	3.94	83.84	90.94	25.51
DeepLabV3	56.98	68.69	32.48	71.56	80.60	23.34	82.80	90.32	15.90	66.57	78.66	8.56	79.84	88.37	21.84
PMRNet (Ours)	64.73	75.51	26.03	73.56	81.88	22.58	82.52	90.17	16.70	86.87	92.74	3.36	85.70	92.03	19.58

Method	ISIC2017			ISIC2018			Kvasir-SEG			PH ²			TN3K		
	IoU↑	Dice↑	HD95↓	IoU↑	Dice↑	HD95↓	IoU↑	Dice↑	HD95↓	IoU↑	Dice↑	HD95↓	IoU↑	Dice↑	HD95↓
UNet	81.68	88.57	16.70	80.73	88.03	20.23	71.68	80.37	45.10	88.07	93.47	18.52	68.68	78.63	30.37
UNet++	81.05	87.98	16.81	81.65	88.81	18.41	76.41	84.02	37.76	89.70	94.46	14.82	70.13	79.71	29.99
TransUNet	82.06	88.85	15.70	80.68	87.90	19.01	78.36	85.64	30.98	89.69	94.39	18.86	70.63	80.20	27.55
Rolling-UNet	82.14	88.82	14.12	81.67	88.76	17.70	76.11	83.88	32.55	89.08	94.08	17.86	70.13	79.77	27.81
EMCAD-B2	81.49	88.29	15.27	81.78	88.74	16.58	78.62	85.85	29.71	89.92	94.58	14.68	72.72	82.02	24.34
Deformable-LKA	78.76	86.02	18.98	82.47	89.26	15.78	77.31	84.37	31.32	90.45	94.90	14.60	67.04	77.69	32.16
DeepLabV3	81.28	88.44	15.56	81.14	88.43	18.04	73.62	81.92	33.04	88.86	93.99	15.05	67.01	77.62	27.59
PMRNet (Ours)	83.14	89.69	13.73	82.51	89.32	15.79	81.21	87.67	26.68	91.07	95.24	14.13	73.50	82.50	23.03

Results: Accuracy & Visualization

- Evaluated on 12 diverse medical imaging datasets.
- Highlights (Clinic Dataset):
 - 87.25% IoU and 92.56% Dice.
- Qualitative Results:
 - Superior boundary delineation.
 - Robust handling of small objects and ambiguous edges.
 - Significant reduction in false positive/negative regions.



Conclusion

- Summary: PMRNet demonstrates that physical inductive biases can effectively replace brute-force parameter scaling.
- Impact: Enables high-accuracy medical image segmentation on resource-constrained devices.
- Open Source: Code is available on GitHub.
- Thank You!

